

# Evidence of Dynamical Constraints Imposed by Water Organization around a Bio–Hydrophobic Interface

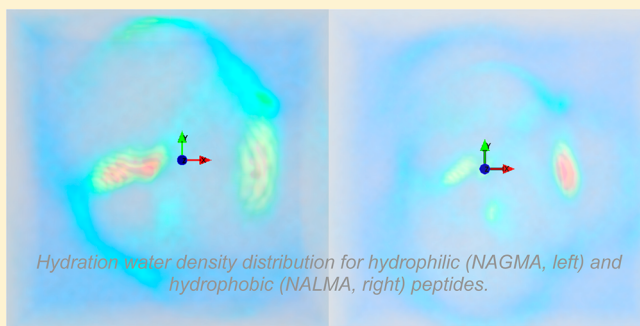
Daniela Russo,<sup>\*,†</sup> Miguel Angel Gonzalez,<sup>‡</sup> Eric Pellegrini,<sup>‡</sup> J. Combet,<sup>‡</sup> J. Ollivier,<sup>‡</sup> and José Teixeira<sup>§</sup>

<sup>†</sup>CNR-IOM c/o Institut Laue Langevin, 6 rue J. Horowitz BP156, F-38042 Grenoble, France

<sup>‡</sup>Institut Laue Langevin, 6 rue J. Horowitz BP156, F-38042 Grenoble, France

<sup>§</sup>Laboratoire Léon Brillouin (CEA/CNRS), CEA Saclay, 91191 Gif-sur-Yvette Cedex France

**ABSTRACT:** Molecular dynamics simulations and elastic neutron scattering experiments have been used to highlight how the structural organization of hydration water is able in some cases to locally constrain atomic movements at biologic interfaces. Using fully hydrated small peptides as models of protein interfaces, we show that the length of the side chains and the hydrophilic backbone have specific signatures. The dynamics of the side chain, which is part of biomolecules, have not only a crucial role in the whole flexibility as compared to the backbone, but also modify the values of transition temperatures. The analysis of the activation energies of methyl group dynamics suggests that the interaction between hydrophobic side chain and surrounding water plays an important role in the whole flexibility as well. We suggest that the progressive water *cluster* organization, around hydrophobic interfaces increases the activation energy and that a plateau regime is reached only when an extended hydrogen-bond network is established. The cluster size corresponds to a single layer of water molecules.



## 1. INTRODUCTION

The role of water molecules in most biological processes does not need to be emphasized. Since pioneering studies as such of G. Careri in the 1980s,<sup>1,2</sup> hydration of proteins and protein dynamics have been studied both experimentally and by computer simulations.<sup>3–18</sup> For example, it is clearly established that a minimum amount of water is necessary for the onset of motions necessary for a biological activity of biomolecules and that the combination of hydration level and temperature generates a large variety of structural and dynamical behaviors. These studies are necessary in particular for the establishment of more general and predictive codes based on a more detailed description at the atomic level, which is still lacking. Such an ambitious goal implies the study of specific representative situations such as the comparison of small peptides differing by a single parameter, the only way to establish the exact role of this parameter on the general dynamics of the peptide. In the past years, we started this kind of studies with the purpose of disentangling the effects of hydrophobic and hydrophilic sites in similar peptides, in particular their extension and interaction with hydration water at different temperatures.<sup>19–23</sup>

In the present contribution, we mainly reconsider two well-studied peptides, *N*-acetyl-leucine-methylamide (NALMA) and *N*-acetyl-glycine-methylamide (NAGMA), which differ by the presence of a hydrophobic chain for the first. Preliminary studies gave essential information about their behavior as a function of water amount (from dry powders to diluted solutions) and of temperature. Here, we focus on the flexibility

and extension of the chains at full hydration level as a function of temperature. We show by neutron elastic scattering and molecular dynamics simulations how, in some conditions, hydration water can constrain local atomic motions at biointerfaces.

## 2. MATERIALS AND METHODS

**2.1. Sample Preparation.** In this study we examine: (a) *N*-acetyl-leucine-methylamide (NALMA), (b) *N*-acetyl-glycine-methylamide (NAGMA), and (c) *N*-acetyl-alanine-methylamide (NALA). All these three peptides share the same polar backbone ( $\text{CH}_3\text{--CO--NH--C}_\alpha\text{H--CO--NH--CH}_3$ ) with  $\text{CH}_3$  end-caps. Instead they differ by the atoms attached to the  $\text{C}_\alpha$  atom, which are: (a) a *hydrophobic* amino acid side chain,  $(\text{CH}_3)_2\text{--CH--CH}_2$ , in the case of NALMA, (b) a hydrogen atom (H), in the case of NAGMA and (c) a  $\text{CH}_3$  group, in the case of NALA. We also consider *L*-Ala, a similar model interface formed by a shorter backbone and a side chain reduced to a  $\text{CH}_3$  group.

These peptides were chosen because their chemical compositions are similar, they share the same hydrophilic backbone and they differ by the size and degree of hydrophobicity of the side chains. The chemical compositions of different peptides are depicted in Figure 1.

**Received:** September 24, 2012

**Revised:** February 12, 2013

**Published:** February 15, 2013

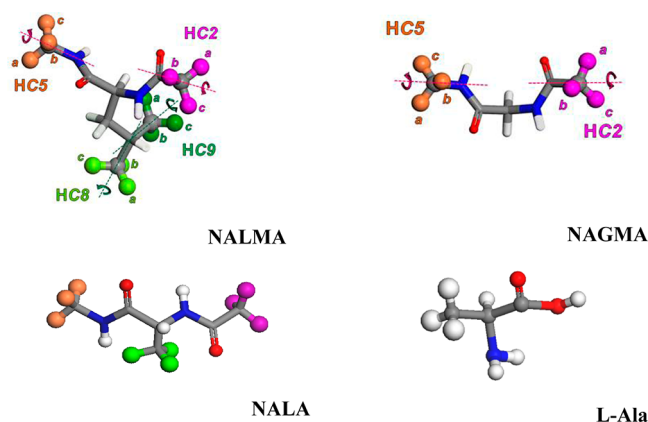


**Figure 1.** Chemical composition of NALMA, NAGMA, NALA, and L-Ala peptides. NALMA and NAGMA methyl groups ( $\text{CH}_3$ ) have been labeled following the adopted molecular dynamics procedure described in section 2.3.

All peptides were completely hydrogenated and they were purchased from Bachem. For the neutron scattering experiments we prepared the samples as follows. First, the peptides, received under the form of powders, were placed under vacuum in presence of silica salts for at least two days in order to be totally dehydrated. Then, deuterated water ( $\text{D}_2\text{O}$ ) was added in well controlled amounts through equilibrium with aqueous solutions with well-defined vapor pressure. The samples are kept for several hours under confined atmosphere together with a salt aqueous solution which have well-defined and almost temperature independent vapor tensions. The total amount of added hydration water was determined by weighting of the samples and is defined by the hydration level, which is the ratio between the mass of water and the mass of the dry peptide ( $h = m_{\text{D}_2\text{O}}/m_{\text{dry sample}}$ ).

Herein we present experimental results obtained with fully hydrated samples, i.e. the highest hydration level before reaching the liquid state. At high hydration level all solutes, still below their solubility level, have a liquid but “opaque” appearance due to precipitations. This corresponds to hydration levels  $h$  equal to the following: (a) 60% (6 water molecules/peptide), for NALMA; (b) 50% (3.3 water molecules/peptide) for NAGMA; (c) 40% (2.6 water molecules/peptide) for NALA; and (d) 40% (2 water molecules/peptide) for L-Ala samples. The  $h$  values have been calculated taking into account the deuterated water molecular weight.

**2.2. Experimental Procedure.** “Elastic scans” neutron scattering experiments have been used to characterize the internal dynamics, flexibility, and dynamical transitions of proteins, focusing on the interface with hydration water.

The choice of heavy water guarantees that almost all the scattered intensity results from the interaction of neutrons with the hydrogen atoms all located on the peptides, because of their very large incoherent cross section. Thus, probing the individual motions of hydrogen atoms, we have a direct access to the dynamics of different segments of the peptides. In this technique only the “elastic” contribution determined by the instrumental resolution is measured. When the diffusive motions of the H atoms are too slow, the corresponding quasi-elastic contribution only contributes as a pure elastic component. However, the measured intensity changes with

temperature, which can be interpreted with the help of appropriate models.

Despite its apparent simplicity, the results of elastic scans are very pertinent and can be interpreted, at least qualitatively, in many cases. However, care must be taken, for example, of the really elastic contribution due to atomic vibrations (the Debye–Waller factor). In contrast, a significant decrease of the (apparently elastic) intensity marks the onset of a relaxation process on the time scale of the instrument. For example, a sharp decrease of the peak intensity can be due to the onset of fast dynamics generating line widths eventually above the experimental resolution. Most of the time, elastic scans are performed as a function of an external parameter, namely temperature. Because the time acquisition is short, it is the large number of experimental results that justifies the final interpretation.

The experiments were performed using the backscattering spectrometer IN16<sup>24</sup> at the Institut Laue Langevin (ILL), with an energy resolution of  $1 \mu\text{eV}$  (that corresponds to a time scale of the order of 700 ps), in a range of temperature between 20 and 310 K. The spectrometer was set in the operational elastic mode (i.e., the Doppler speed of the monochromator was set equal to zero), the collected signal was measured over a wave vector  $Q$  range extending from  $0.2$  to  $1.89 \text{ \AA}^{-1}$  (where  $Q = (4\pi \sin \theta)/\lambda$  is the elastic momentum exchange,  $2\theta$  is the scattering angle, and  $\lambda$  is the wavelength of the incident neutrons).

All the elastic scans, performed as a function of temperature, were recorded using a heating rate of  $0.5 \text{ K/min}$  and an acquisition time equal to  $3 \text{ min/point}$ . A typical elastic scan collection time was of the order of  $12 \text{ h}$  per sample. All samples were loaded into slab containers  $0.5 \text{ mm}$  thick. All spectra were corrected for detector efficiencies and normalized to their  $20 \text{ K}$  temperature scans, using the ILL LAMP programs.<sup>25</sup> The evaluation of the  $Q$  dependence of the scattered intensity gives access to the mean square displacement of hydrogen atoms as a function of temperature. The intensity of the signal and the experimental resolution does not allow any unambiguous study of the signal, which reduces to an apparent elastic peak. To minimize the data manipulation we decided to proceed with the intensity analysis.

**2.3. Computational Details.** Molecular Dynamics simulations were performed using the Forcite module provided in Materials Studio 5.0<sup>26</sup> with the COMPASS 27 force field.<sup>27</sup> The structures of NALMA and NAGMA peptides have been initialized using atomic positions reported in crystallographic studies.<sup>28,29</sup> Each of the  $n$  hydration water molecules was added step by step, and the optimized geometry of the single unit (peptide: $n$  water) has been calculated. Then, the (peptide: $n$  water) unit was replicated to generate amorphous packs of peptides, using the Theodorou/Suter method, as implemented in the Amorphous-Cell module. The density of the system at each studied hydration has been calculated by interpolation based on the polynomial fitting of data obtained between the pure crystal<sup>28,29</sup> and concentrated solutions.<sup>30,31</sup> Two simulation boxes, containing either 72 NALMA and 504 water molecules or 100 NAGMA and 400 water molecules, were prepared and initially equilibrated in the NVT ensemble during  $260 \text{ ps}$  with a time step of  $1.0 \text{ fs}$ , and using Berendsen’s thermostat with a relaxation constant of  $1.0 \text{ ps}$ . Three-dimensional cubic periodic boundary conditions were applied, and a cutoff of  $10 \text{ \AA}$  was employed to compute the van der Waals interactions. The Ewald summation was used to treat the long-range electrostatic interactions. The equilibration run was

followed by a production run of 1 ns performed also in the NVT ensemble under the same conditions.

Herein we consider NALMA and NAGMA trajectories calculated at temperatures between 150 and 298 K and at hydration levels between 0 and 67%. We remark that the  $h$  values have been calculated considering the molecular weight of light water. It follows that they will differ from the reported experimental values and that the comparison must be done by comparing the number of water molecules/peptide. Table 1 reports the  $n/h$  corresponding values.

**Table 1**

water molecules for NAGMA molecule (MW 130 amu)	$h$ (%)	water molecules for NALMA molecule (MW 186 amu)	$h$ (%)
0.6	8.3	1	9.6
1	13.8	2	19.3
2	27.6	3	29
3	41.5	7	67.7
4	55.3		

The program nMOLDYN v3.4<sup>32</sup> has been used to analyze the trajectories, in particular to evaluate the rotational autocorrelation function of hydrogen atoms of different methyl groups in the peptides which are labeled in accordance with Figure 1. The hydrophilic peptide NAGMA has two methyl groups located at the end caps of the backbone tagged HC2 and HC5. In addition to these end groups, the hydrophobic peptide NALMA also owns side-chain methyl groups which have been labeled HC8 and HC9.

The angular correlation analysis computes the dynamics of rotations around the three orthogonal vectors attached to CH<sub>3</sub> groups. Considering the function  $C_i(t) = \langle v_i(0) \cdot v_i(t) \rangle$ , where  $v_i(t)$  is one of the orthonormal position vectors ( $i = 1-3$ ), we defined two orthonormal vectors in the plane of the three hydrogen atoms of a methyl group, generating the correlation functions  $C_1(t)$  and  $C_2(t)$ , and one orthogonal to this one generating  $C_3(t)$ . The axes are schematically shown as red, green, and blue, respectively, in the insets of Figure 4. The CH<sub>3</sub> carbon position has been defined as the origin of the vectors. As a consequence of this definition, somehow the correlation function  $C_3(t)$  is related to the global rotation of the peptide, for HC2 and HC5 (the backbone), and to the local side-chain diffusive relaxation for the HC8 and HC9.

By symmetry,  $C_1(t) = C_2(t)$ ; assuming  $v_1$  and  $v_2$  are independent, both  $C_1(t)$  and  $C_2(t)$  are proportional to the methyl group reorientation ( $C_{Me}(t)$ ) convoluted to  $C_3(t)$  ( $C_1(t) = C_2(t) = C_{Me}(t) * C_3(t)$ ). Since the  $C_i(t)$  can be satisfactorily adjusted using a single exponential form and taking into account that the global rotation of the whole molecule is several orders of magnitude slower ( $\tau_3 =$  nano-second time scale, Figure 3) than the rotations of methyl groups, we assumed to a first approximation that the backbone methyl rotational relaxation time  $\tau_{Me}$  (ps) is equal to  $\tau_1$  (taking into account that  $\tau_{Me}^{-1} = \tau_1^{-1} - \tau_3^{-1}$  where  $\tau_3 \gg \tau_1$ ).

The intermolecular and intramolecular density distribution, of hydration water and peptide selected atoms, have been also calculated, following the method described by Aoun and co-workers.<sup>33</sup> This complementary information allows a more precise interpretation of the autocorrelation function.

### 3. RESULTS AND DISCUSSION

Our study of the slow motions and flexibility of the peptides is based on a detailed interpretation of the temperature dependence of elastic scans. With the help of computer simulations of the molecular dynamics, it is possible in many cases to disentangle the contributions coming either from the backbone or from the different side chains. For this purpose, our experiments and simulations concern mainly NALMA and NAGMA peptides studied in detail in our previous work as well as NALA, a similar molecule with the same backbone as the former two but with a side chain reduced to a methyl group generating a localized hydrophobic site. As explained above, in order to deepen our knowledge on the importance of backbone length we also consider the short single amino acid L-Ala.

**Neutron Scattering Experiments.** Figure 2 shows the integrated elastic intensity (IEI, summed up to  $Q = 1.4 \text{ \AA}^{-1}$  in

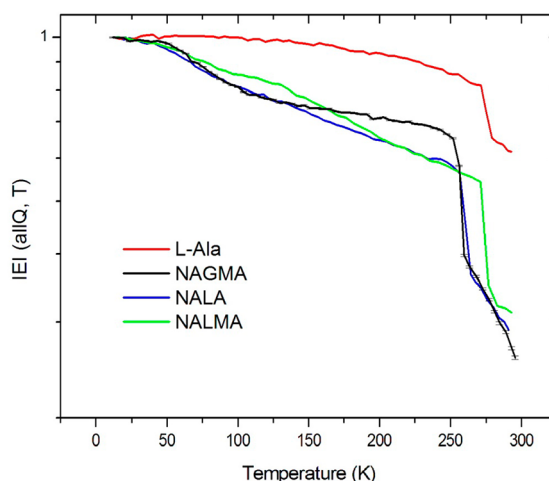


**Figure 2.** Integrated elastic intensity as a function of temperature for fully hydrated peptides ( $h = 50\%$  for NAGMA,  $60\%$  for NALMA,  $40\%$  for NALA, and  $40\%$  for L-Ala).

order to avoid the water Bragg peak region) as a function of temperature for NALMA, NAGMA, and NALA fully hydrated peptides together with the fully hydrated single amino acid L-Ala. Error bars are represented only for the NAGMA curve and are representative for all curves. All the curves exhibit the same general trend: a smooth decrease at lower temperatures followed by an abrupt drop of the integrated intensity above 250 K. Part of the small continuous decrease of intensity is due to the increasing amplitude of atomic and molecular vibrations, which are harmonic to a first approximation, while larger slopes and discontinuities are representative of significant changes of the dynamics of the samples. We notice first that the slope is significantly higher for all peptides with an extended backbone (all the NA-xx-A) as compared to the short amino acid (L-Ala).

We can compare in more detail the curves obtained for L-Ala and NALA as both samples have in common a side chain reduced to a CH<sub>3</sub> group but differ by the length of the main chain. Also, the number of water molecules at full hydration is almost the same for both molecules.

The very different temperature dependence in each case demonstrates that the length and associated flexibility of the backbone plays a major role in the dynamics of the two molecules. At the lowest temperature, NALA shows an important decrease of elastic intensity as compared to that of



the L-Ala, for which the temperature dependence of the scattered intensity is almost null between 50 and 100 K.

The very small decrease of elastic intensity in the case of L-Ala may be associated to a different hydration water network or to an intrinsic rigidity of the molecule. Despite an equivalent hydration level (2–3 water molecules/peptide), the different lengths of the two peptides and the presence of a local charge at the terminals of L-Ala influence the local water arrangement. Likely, hydration water around L-Ala starts the formation of a cage that *enhances* the global rigidity of the molecule and in some way hampers the dynamics of the CH<sub>3</sub> side chain in addition to a non-negligible shift of about 20 K of the temperature of the drop of intensity. In a previous work we also observed<sup>34</sup> that, in the 80 ps time scale, there are no differences of IEI between dry and hydrated L-Ala ( $Q$  range up to 5 Å<sup>-1</sup>) before the dynamical transition. The temperature dependence suggests that water–peptide interaction is not only responsible for the extremely rigid behavior. It is plausible that the length of L-Ala corresponds to the length defining the short distance interactions, reflecting the rigidity of the chain. This length depends on the chemical structure of the molecule<sup>35</sup>

Comparing all the peptides that share the same hydrophilic backbone length at equivalent hydration level, we identify two main regions: one between 70 and 250 K and the other above 250 K. In the latter, a sharp transition is observed in all cases, which corresponds obviously to the onset of diffusive motions. Despite the fact that hydration water is fully deuterated, one cannot exclude a small contribution due to the melting of small inclusions of ice. However, while for NALMA, which includes a hydrophobic side chain, the transition takes place at 270 K as for the rigid L-Ala, for the other samples (NAGMA and NALA), it happens at a lower temperature (255 K). Recall that for these two samples the place of the side chain is occupied either by a single hydrogen atom (NAGMA) or by a methyl group (NALA).

The values of the transition temperatures are under the melting temperature of pure bulk water (277 K). Although the notion of melting should not be applied to a single layer of water, it is expected that, in a situation of confinement, diffusion motions take place at lower temperatures as the melting temperature is also depressed in confined volumes of liquids. The extended network of hydrogen bonds formed near the side chain in the case of NALMA delays the onset of translational motions.

We interpret this discriminating temperature behavior by the fact that the hydrophobic chain of NALMA generates a relatively extended network of hydrogen-bonded water molecules sitting preferentially parallel to the chain, that substantially increases its rigidity. The stability of the water bonds and the extension of the resulting network prevent part of the diffusive motions of the chain.

Only at temperatures large enough to disrupt the water network increasing its own mobility is the chain flexible enough to generate a quasi-elastic intensity. In the other cases, either the hydrophobic character is not present (NAGMA) or its extension is reduced to a single CH<sub>3</sub> group (NALA), which is not sufficient to generate visible effects on the surrounding water dynamics. This is actually the case of other molecules containing methyl groups soluble in water, as for example DMSO.<sup>36</sup>

Generally speaking, in a hydrophilic environment, mobility of water with increasing temperature takes place smoothly by gradual steps from breaking of hydrogen bonds, local jumps,

individual rotations, and then molecular diffusion, while in an extended hydrophobic environment, a network of intermolecular water hydrogen bonds remains intact up to higher temperatures and breaks suddenly around 270 K. Consequently, the effect of a hydrophobic region of the peptide can be observed in the transition temperature only if the extension of the hydrophobic region is large enough to generate an extended network of hydrogen bonds between water molecules.

However, the picture can be more complex. In a previous work<sup>23</sup> we have shown that, at room temperature and in highly concentrated solutions when the NALMA peptide is surrounded by a single hydration shell, the hydrophobic side chain is also constrained in its diffusive motions. It follows that a large extension of the hydrogen bond balances the high temperature effect on the activation of diffusive motions.

In the temperature range below 250 K, where all samples except L-Ala show a significant decrease of the elastic intensity, we can also discriminate among different behaviors. In temperatures up to 70 K all curves show an intensity decrease starting at 50 K, the onset of methyl group dynamics. Above 70 K, whereas NALA and NAGMA exhibit the same temperature dependence up to 130 K, NALMA shows weaker temperature dependence up to 200 K, a behavior that can be understood as the manifestation of a higher rigidity resultant from the presence of its hydrophobic side chain. However, in this range of temperature, a contribution of the hydration water caging effect around the side chain is not excluded, .

From 200 to 250 K the dynamics of NALA and NALMA, both with a side chain including a CH<sub>3</sub> group, match again. Also in this case it is interesting to notice that this range of temperature corresponds to the range where, in average, the protein dynamic transition occurs.

Another interesting temperature to discuss is 130 K. Zanotti<sup>37,38</sup> and co-workers demonstrated that this temperature corresponds to the onset of rotational relaxation dynamics of confined water molecules. In our case we observe that, exactly at this temperature, the elastic intensities of NALA (hydrophilic backbone, CH<sub>3</sub>-side chain) and NAGMA (hydrophilic backbone, H-side chain) start to diverge, showing more rigid backbone dynamics up to the dynamical transitions. This behavior arises from a combination of a lack of a side chain and a more pronounced water *slaving effect* given the formation of strong backbone–water interactions (as it appears from the density distribution represented in the TOC).

On one side, we highlight that combining the water caging effect around a hydrophobic biointerface to its extension introduces a constraint on the mobility of the molecule up to 200–230 K, the temperature at which the water translational diffusion starts.<sup>38</sup> On the other side, the high-density water structure around the hydrophilic backbone makes the peptide dynamics weakly dependent on temperature when the rotational motions of water take place.

**2. Molecular Dynamics Simulations.** A supplementary argument of our interpretation is provided by molecular dynamics simulations (MD).

First we calculate the intramolecular density distribution in NALMA. Fixing the origin of the Cartesian axes at the C<sub>α</sub> carbon and defining the  $X$  axis on the C<sub>α</sub>–N1 direction, we observed that the spatial distribution of the hydrogen atoms of the backbone methyl groups are more delocalized than those of the side chain (Figure 3). In agreement, we also remark that the carbon atoms of the CH<sub>3</sub> are more delocalized at the backbone than at the extremity of the side chain, suggesting a higher

amplitude of motions and a reduced spatial geometric constraint. It is worth stressing that global diffusion and rotation are not contributing to the density map.

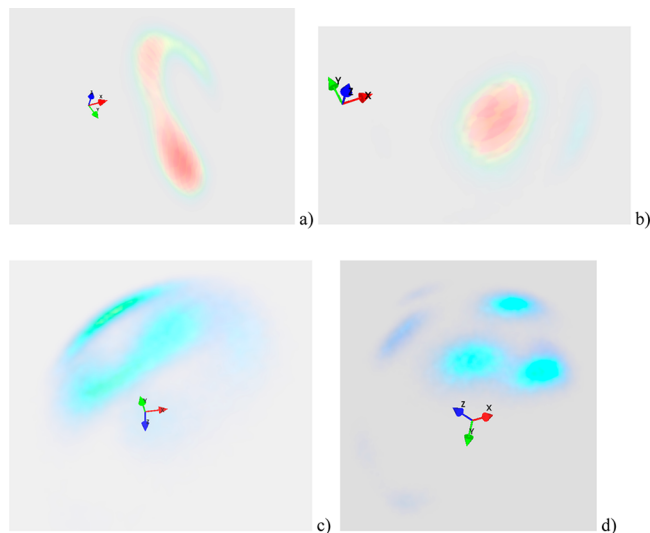


**Figure 3.** Intramolecular density distribution of carbon atoms (a, b) and hydrogen atoms (c, d) of the methyl group at the backbone (a, c) and side chains (b, d). (a) C2, (b) C8, (c) HC2, (d) HC8.

We calculate the rotational autocorrelation function of each methyl group at the extremities of the hydrophilic backbone (Figure 1, groups HC2 and HC5) and at the extremity of the NALMA side chain (Figure 1, groups HC8 and HC9). As previously anticipated, the rotation of the whole molecule is decorrelated from the  $\text{CH}_3$  dynamics for what concerns the backbone analysis. However, for the side chain analysis,  $C_3(t)$  is mostly correlated to the local rearrangement of the side-chain. We estimate that this contribution does not hamper our analysis. Figure 4 shows the typical behavior of  $C_1(t) = C_2(t)$  and  $C_3(t)$  autocorrelation functions at room temperature.  $C_1(t)$  describes the mobility of methyl groups, and therefore, it decays much faster than  $C_3(t)$ . It follows that we concentrate our attention only on  $C_1(t)$ .

Figure 5a shows an example of the calculated rotational autocorrelation function  $C_1(t)$ , at 200 and 298 K, for the NALMA sample hydrated by 7 molecules of water (67%). We observe that the temperature dependence is in agreement with the experimental results, confirming that the dynamics associated to the methyl groups of the side chain are much slower than those of the methyl groups of the backbone. The first thought could be that the compared functions are not exactly the same: in the case of the side chain (HC8),  $C_1(t) = C_{\text{Me}}(t) * C_3(t)$ , mostly at short times (Figure 5a), while for the backbone we have  $C_1(t) = C_{\text{Me}}(t)$ . However, a more realistic possibility could be that this effect can be explained by the combination of two contributions such as a geometrical constraint and/or a dynamical coupling. Indeed, it is possible that the vicinity of the two methyl groups attached to the side chain through the same carbon atom, combined with the hydration water structural organization, generates a coupling that slows down their dynamics. Those results are in agreement with what was observed through the calculation of intermolecular density distributions.

Analyzing the low temperature hydration dependence we also found an anomalous behavior. Parts b and c of Figure 5

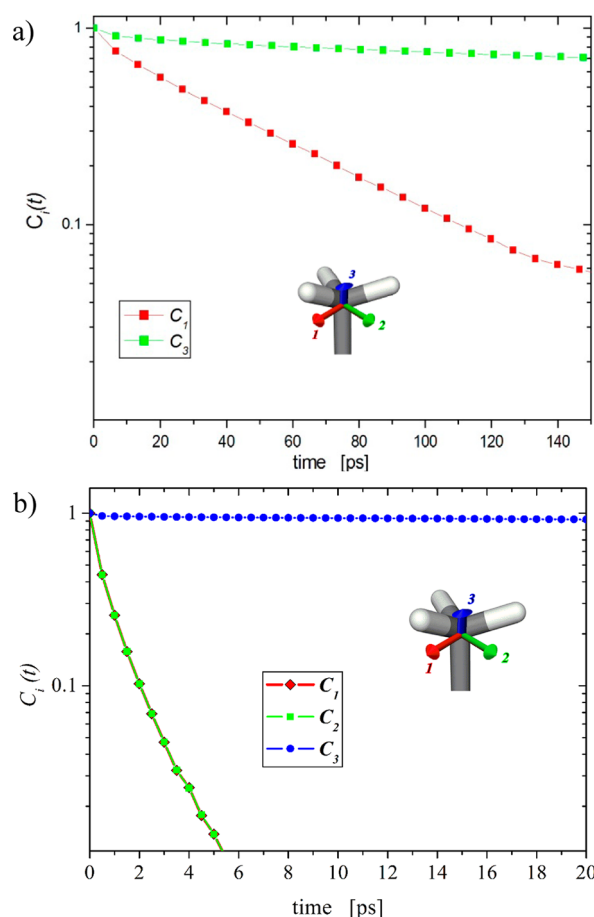


**Figure 4.** Example of comparison of  $C_1(t)$  and  $C_3(t)$  autocorrelation functions evaluated at room temperature for (a) HC8 for 1 NALMA:3  $\text{H}_2\text{O}$  and (b) HC2 for 1 NALMA:7  $\text{H}_2\text{O}$ . Note the two different time scales.

represent the hydration dependence at 200 K of NALMA methyl groups identified in Figure 1. For the group HC8 of the side chain (Figure 5b), higher is the hydration level and slower is the relaxation. We observed that this behavior persists up to 270 K when the energy provided by the temperature promotes a “more normal” direct correlation between the hydration level and a faster relaxation time. On the other hand, a different and opposite trend is observed for the HC2 methyl groups at the extremities of the backbone (Figure 5c), for which a slower relaxation is observed at low hydration.

All the autocorrelation functions have been adjusted to single exponentials, in order to extract the rotational correlation time  $\tau$ . We observe 1 order of magnitude difference between the relaxation times of methyl groups of the side chain and those of the backbone. According to Figure 5a), we probed these relaxation times as a function of temperature and hydration level. From the temperature dependence, we extracted the activation energies for the investigated HC2, HC5 (for both peptides) and HC8 and HC9 motions, at different hydration levels (Figure 6). Activation energy values have been obtained from Arrhenius plots of relaxation times analyzed in the temperature range between 150 and 300 K. The results show without ambiguity that the dynamics of the methyl groups of the side chain depend on hydration. In contrast, the dynamics of the methyl groups of the backbone are independent of the hydration level. The dependence on hydration level of the side

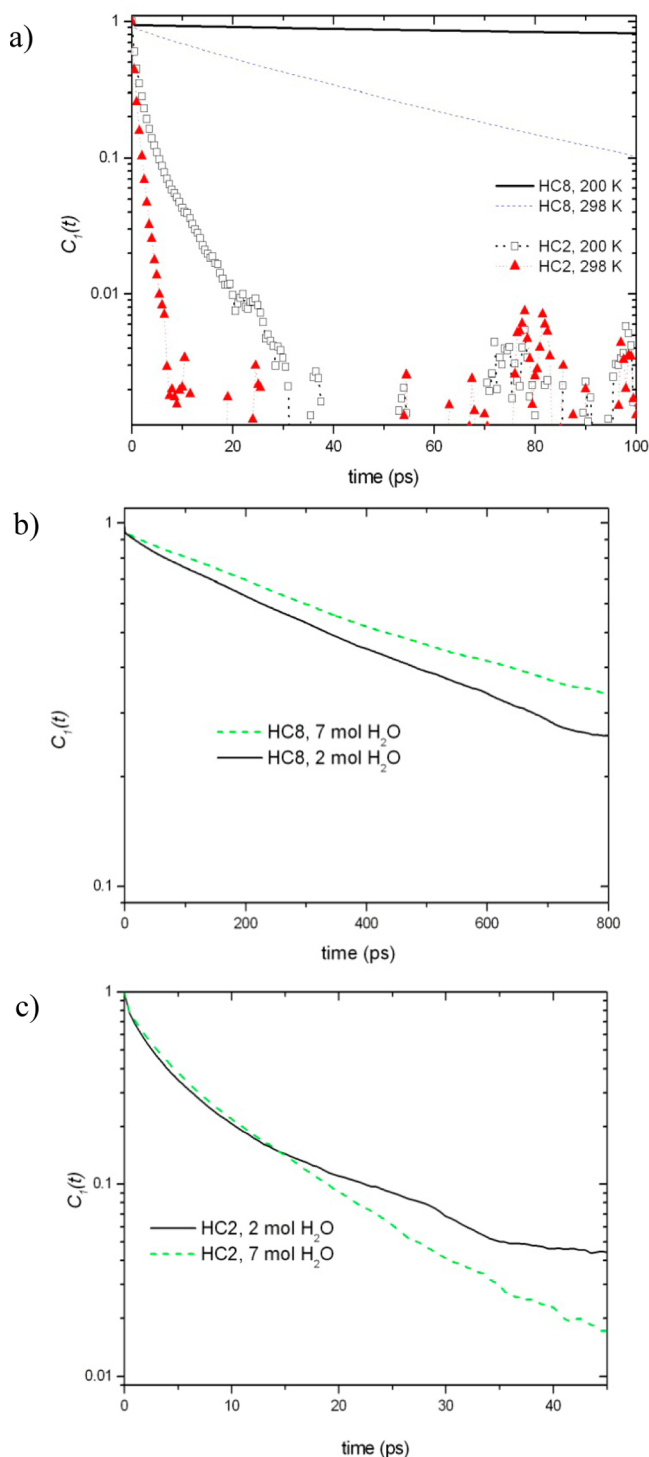


**Figure 5.** HC2 (backbone) and HC8 (side-chain) methyl group autocorrelation function for NALMA peptide as a function of temperature and hydration level: (a) comparison of HC2 and HC8 as a function of temperature at the hydration level of 7 water molecules; (b) comparison of HC8 autocorrelation functions, at 200 K, as a function of hydration level; (c) comparison of HC2 autocorrelation functions, at 200 K, as a function of hydration level.

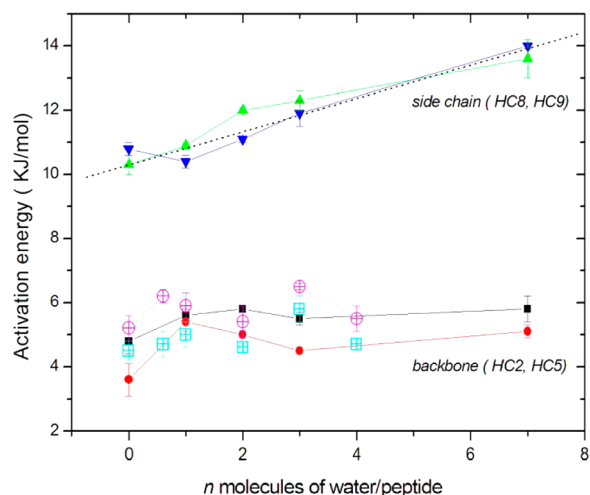


**Figure 6.** Activation energy as a function of the number of water molecules/peptide, extracted from the temperature dependence of the rotational relaxation times. Blue and green triangles represent respectively HC8 and HC9 activation energy. The red circles and black squares represent the HC2 and HC5 values of NALMA, respectively, while crossed circles and crossed squares represent those of the NAGMA values, respectively.

chain methyl group dynamics naturally lead to the interpretation that interaction between the hydrophobic side chain and the surrounding water plays an important role. It is likely that an increase of the hydration level corresponds to an increase of activation energy because of the water cluster organization around the hydrophobic NALMA side chain and its *coupling* with the methyl groups.

The average value of the activation energy is 5.5 kJ/mol for the backbone methyl groups and 12 kJ/mol for the side chain groups. Activation energy values between 4 and 12 kJ/mol are comparable to the energy of intermolecular bonds between water molecules which is of the order of 8 kJ/mol which emphasizes the mutual interaction between motions of parts of the protein and water dynamics. These results are in excellent agreement with previous neutron, molecular dynamics, and NMR studies of methyl group dynamics.<sup>23,39–41</sup> In particular, it is worth remarking that D. Russo and co-workers estimated<sup>23</sup> for the NALMA methyl groups in high concentrated solutions, an average activation energy equal to 8.7 kJ/mol. If we think in terms of a rough average between the side chains and a constant backbone, we obtain a value for the activation energy of 15 kJ/mol for the methyl groups of the side chains in the 2 M solution (corresponding to 25 water molecules/peptide). A possible interpretation is that increasing the number of hydration water molecules results in the activation energy reaching a plateau and then a regime independent of hydration. This view is based on the idea that a higher plasticity of the hydrogen-bond network is reflected in a reduced steric constraint and methyl coupling effect. The plateau likely corresponds to the formation of a cluster of about one layer of water molecules at the hydrophobic interface.

#### 4. CONCLUSION

In a general picture, where all the biomolecules are equally hydrated and exposed to the solvent, we observe that the lengths of the hydrophobic side chains and that of the hydrophilic backbone have a different and specific signature. We are unable to distinguish this peculiar fingerprint in a whole



protein except if a selective deuteration could be performed. We also observe that, in the protein dynamical region, the dynamics of the side chain has a more important role in the whole flexibility than the backbone and it affects the transition temperature. The presence of a fully hydrated and extended hydrophobic interface also seems to affect the local dynamics promoting the level of rigidity. It is possible that, for different proteins, the small differences between transition temperatures can be related to the respective amount of hydrophobic/-philic residues present at the surface of the protein.

Another aspect which is worth mentioning is the presence of a transition not only in peptides without side chains but also in a simple amino acid. This property suggests not only that side chains are not necessary in order for the dynamical transition to occur, but also that the length of a polypeptide chain is not a pertinent factor. Finally, once more our results prove that the onset of a transition and large amplitude motions can be considered as physical characteristics of biomolecules related to hydration water and independent of the protein function and structure.

## AUTHOR INFORMATION

### Corresponding Author

\*E-mail: russo@ill.fr

### Notes

The authors declare no competing financial interest.

## ACKNOWLEDGMENTS

D.R. thanks Institut Laue Langevin (ILL) for beam time allocation on the IN16 backscattering instrument, S. Perticaroli for her contribution to the calculation of MD trajectories, and B. Aoun for the calculation of the inter- and intramolecular density distributions.

## REFERENCES

- (1) Rupley, J. A.; Careri, G. Protein Hydration and Function. *Adv. Protein Chem.* **1991**, *41*, 37–172.
- (2) Rupley, J. A.; Gratton, E.; Careri, G. Water and Globular Protein. *Trends Biochem. Sci.* **1983**, *8*, 18–22.
- (3) Wang, Y.; Schwieters, C. D.; Tjandra, N. Parameterization of Solvent-Protein Interaction and Its Use on NMR Protein Structure Determination. *J. Magn. Reson.* **2012**, *221*, 76–84.
- (4) Ebbinghaus, S.; Meister, K.; Prigozhin, M. B.; DeVries, A. L.; Havenith, M.; Dzubiella, J.; Gruebele, M. Functional Importance of Short-Range Binding and Long-Range Solvent Interactions in Helical Antifreeze Peptides. *Biophys. J.* **2012**, *103* (2), L20–L22.
- (5) Chong, S. H.; Ham, S. Impact of Chemical Heterogeneity on Protein Self-assembly in Water. *Proc. Natl. Acad. Sci. U.S.A.* **2012**, *109* (20), 7636–7641.
- (6) Ramakrishnan, V.; Rajagopalan, R. Dynamics and Thermodynamics of Water Around EcoRI Bound to a Minimally Mutated DNA Chain. *Phys. Chem. Chem. Phys.* **2012**, *14* (35), 12277–12284.
- (7) Combet, S.; Zanotti, J.-M. Further Evidence that Interfacial Water is the Main “driving force” of Protein Dynamics: A Neutron Scattering Study on Perdeuterated C-Phycocyanin. *Phys. Chem. Chem. Phys.* **2012**, *14*, 4927–4934.
- (8) Qvist, J.; Ortega, G.; Tadeo, X.; Millet, O.; Halle, B. Hydration Dynamics of a Halophilic Protein in Folded and Unfolded States. *J. Phys. Chem. B* **2012**, *116*, 3436–3444.
- (9) Capaccioli, S.; Ngai, K. L.; Ancherbak, S.; Paciaroni, A. Evidence of Coexistence of Change of Caged Dynamics at T-g and the Dynamic Transition at T-d in Solvated Proteins. *J. Phys. Chem. B* **2012**, *116*, 1745–1757.
- (10) Russo, D.; Orecchini, A.; De Francesco, A.; Laloni, A.; Petrillo, C.; Sacchetti, F. Brillouin Neutron Spectroscopy as a Probe to Investigate Collective Density Fluctuations in Biomolecules Hydration Water. *Spectrosc. Int. J.* **2012**, *27*, 293–305.
- (11) Mallamace, F.; Corsaro, C.; Mallamace, D.; Baglioni, P.; Stanley, H. E.; Chen, S.-H. Water in the Protein Folding Process. *J. Phys. Chem. B* **2011**, *115*, 14280–14294.
- (12) Armstrong, B. D.; Choi, J.; Lopez, C.; Wesener, D. A.; Hubbell, W.; Cavagnero, S.; Han, S. Site-Specific Hydration Dynamics in the Nonpolar Core of a Molten Globule by Dynamic Nuclear Polarization of Water. *J. Am. Chem. Soc.* **2011**, *133*, 5987–5995.
- (13) Zhong, D. P.; Pal, S. K.; Zewail, A. H. Femtosecond Dynamics of a Drug-Protein Complex: Daunomycin with Apo Riboflavin-Binding Protein. *Chem. Phys. Lett.* **2011**, *503*, 1–11.
- (14) Roh, J. H.; Tyagi, M.; Briber, R.; M.; Woodson, S. A.; Sokolov, A. P. The Dynamics of Unfolded Versus Folded tRNA: The Role of Electrostatic Interactions. *J. Am. Chem. Soc.* **2011**, *133*, 16406–16409.
- (15) Fujiwara, S.; Plazanet, M.; Matsumoto, F.; Oda, T. Internal Motions of Actin Characterized by Quasielastic Neutron Scattering. *Eur. Biophys. J. Biophys. Lett.* **2011**, *40*, 661–671.
- (16) Stadler, A. M.; van Eijck, L.; Demmel, F.; Artmann, G. Macromolecular Dynamics in Red Blood Cells Investigated Using Neutron Spectroscopy. *J. R. Soc. Interface* **2011**, *8* (57), 590–600.
- (17) Jasnin, M.; van Eijck, L.; Koza, M. M.; Peters, J.; Laguri, C.; Lortat-Jacob, H.; Zaccari, G. Dynamics of Heparan Sulfate Explored by Neutron Scattering. *Phys. Chem. Chem. Phys.* **2010**, *12* (14), 3360–3362.
- (18) Russo, D.; Perez, J.; Zanotti, J. M.; Desmadril, M.; Durand, D. Dynamic Transition Associated with the Thermal Denaturation of a Small Beta Protein. *Biophys. J.* **2002**, *83* (5), 2792–2800.
- (19) Russo, D.; Copley, J.; Ollivier, J.; Teixeira, J. On the Behaviour of Water Hydrogen Bonds at Biomolecular Sites: Dependences on Temperature and on Network Dimensionality. *J. Mol. Struct.* **2010**, *972*, 81–86.
- (20) Russo, D.; Ollivier, J.; Teixeira, J. Water Hydrogen Bond Analysis on Hydrophilic and Hydrophobic Bio-molecules Sites. *Phys. Chem. Chem. Phys.* **2008**, *10*, 4968–4974.
- (21) Russo, D.; Teixeira, J.; Kneller, L.; Copley, J. R. D.; Ollivier, J.; Perticaroli, S.; Pellegrini, E.; Gonzalez, M. A. Vibrational Density of States of Hydration Water at Biomolecular Sites: Hydrophobicity Promotes Low Density Amorphous Ice Behaviour. *J. Am. Chem. Soc.* **2011**, *133*, 4882–4888.
- (22) Russo, D. The Impact of Kosmotropes and Chaotropes on Bulk and Hydration Shell Water Dynamics in a Model Peptide Solution. *Chem. Phys.* **2007**, *345*, 200–211.
- (23) Russo, D.; Hura, G.; Copley, J. D. R. Effects of Hydration Water on Protein Methyl Group Dynamics in Solution. *Phys. Rev. E* **2007**, *75*, 040902.
- (24) <http://www.ill.eu/instruments-support/instrumentgroups/instruments/in16/>
- (25) <http://www.ill.eu/instruments-support/computing-for-science/cs-software/all-software/lamp/the-lamp-book/>
- (26) *Materials Studio: Materials Modelling and Simulation*, v. 5.0; Accelrys Inc.: San Diego, CA, 2009.
- (27) Sun, H. COMPASS: An ab Initio Force-Field Optimized for Condensed-Phase Applications Overview with Details on Alkane and Benzene Compounds. *J. Phys. Chem. B* **1998**, *102*, 7338–7364.
- (28) Iwasaki, G. Acetylglycine-N-methylamide. *Acta Crystallogr., Sect. B* **1974**, *30*, 2503–2505.
- (29) Ichikawa, T.; Iitaka, Y. The Crystal Structure of DL-Acetylucine N-Methylamide, C<sub>9</sub>H<sub>18</sub>O<sub>2</sub>N<sub>2</sub>. *Acta Crystallogr., Sect. B* **1969**, *25*, 1824–1833.
- (30) Leslie, T. E.; Lilley, T. H. Aqueous Solutions Containing Amino Acids and Peptides. Part 20. Volumetric Behavior of Some Terminally Substituted Amino Acids and Peptides at 298.15 K. *Biopolymers* **1985**, *24*, 695–710.
- (31) Perticaroli, S. PhD thesis, University of Perugia: Perugia, Italy, 2011.
- (32) Hinsen, K.; Pellegrini, E.; Stachura, S.; Kneller, G. nMoldyn 3: Using Task Farming for a Parallel Spectroscopy-Oriented Analysis of

Molecular Dynamics Simulations. *J. Comput. Chem.* **2012**, *33*, 2043–2048.

(33) Aoun, B.; Gonzalez, M. A.; Ollivier, J.; Russina, M.; Izaola, Z.; Price, D. L.; Saboungi, M. L. Translational and Reorientational Dynamics of an Imidazolium-Based Ionic Liquid. *J. Phys. Chem. Lett.* **2010**, *1*, 2503–2507.

(34) Russo, D.; Ollivier, J.; Teixeira, J. The Impact of Hydration Water on the Dynamics of Side Chains of Hydrophobic Peptides: From Dry Powder to Highly Concentrated Solutions. *J. Chem. Phys.* **2009**, *130*, 235101–9.

(35) Sharp, P.; Bloomfield, V. A. Light Scattering from Wormlike Chains with Excluded Volume Effects. *Biopolymers* **1968**, *6*, 1201–1211.

(36) Cabral, J. T.; Luzar, A.; Teixeira, J. Water Dynamics in DMSO-Water Mixture. *Physica B* **2000**, *276*, 508–509.

(37) Zanotti, J.-M.; Bellissent-Funel, M.-C.; Kolesnikov, A. I. Phase Transitions of Interfacial Water at 165 and 240 K. Connections to Bulk Water Physics and Protein Dynamics. *Eur. Phys. J. – Spec. Top.* **2007**, *141*, 227–233.

(38) Zanotti, J.-M.; Bellissent-Funel, M.-C.; Chen, S. H. Experimental Evidence of a Liquid-Liquid Transition in Interfacial Water. *Europhys. Lett.* **2005**, *71*, 91–97.

(39) Krishnan, K.; Kurkal-Siebert, V.; Smith, J. C. Methyl Group Dynamics and the Onset of Anharmonicity. *J. Phys. Chem. B* **2008**, *112*, 5522–5533.

(40) Beshah, K.; Olejniczak, E. T.; Griffin, R. G. Deuterium NMR Study of Methyl Group Dynamics in *L*-alanine. *J. Chem. Phys.* **1987**, *86* (10), 5411–5420.

(41) Chatfield, D. C.; Wong, S. E. Methyl Motional Parameters in Crystalline *L*-Alanine: Molecular Dynamics Simulation and NMR. *J. Phys. Chem. B* **2000**, *104*, 11342–11348.

## ■ EDITOR'S NOTE

Following the large amount of literature on the hydration water and protein dynamics and the impossibility to cite all those works in the introduction, the authors decided to refer as much as possible to latest publications sampling in different techniques.